International Research Journal of Natural and Applied Sciences
ISSN: (2349-4077)
Impact Factor 7.032 Volume 10, Issue 03, March 2023
Website- www.aarf.asia, Email : editor@aarf.asia , editoraarf@gmail.com

FREEZING TRANSITIONS IN A TWO-DIMENSIONAL SYSTEM OF MODEL ULTRASOFT COLLOID AND PAIR CORRELATION FUNCTIONS

Anuj Kumar

Research Scholar

Dr Nand Kumar

Professor

Shri krishna university, chhatarpur(M.P.)

ABSTRACT

The radial distribution functions g(r) for the system of psections that interact through a Hertzian potential with an exponent η equal to 5/2 are compared with the results from experiments and molecular dynamics simulations reported in Reference. These numbers correspond to scaled number densities. Additionally, a strength parameter of 496kBT is included in the analysis. In spite of the fact that HNC is often linked with psection systems that have long-range interaction potentials, it has been shown to be successful in this specific instance of core-softened potentials. PY IET, on the other hand, produces exceptional results when applied to hard potentials that are sort-ranged. For the purpose of allowing you to evaluate the performance of HNC in comparison to that of PY closure, we have also provided the PCF curves that were generated by PY IET. There is a significant degree of qualitative agreement between the experimental curves and the simulation curves, and the g(r) that was computed using HNC and PY IETs is practically identical to both of them. It is seen that the HNC considerably underestimates the correlations as we go from low densities to high densities; nonetheless, while we are at low densities, the agreement is remarkable in terms of its quantitative quality.

Keywords :- Freezing, Transitions, Ultrasoft, Colloid

INTRODUCTION

The term colloid describe supramolecular entities whose extension, at least in one spatial dimension, lies between 1 nm ~ 1μm. Therefore, not only spherical but also ellipsoidal sections in solution, platelets and rods in suspension as well as micro gels, vesicles and biomaterials can be classified as colloidal system. They are most common in chemical, pharmaceutical, agriculture and food industries and offer a playground for various statistical

mechanical phenomena because of the ease of inducing spectacular changes in the effective intersection interactions, changing the quality of solvent, temperature, salt concentration or in the chemistry of the components. In order to facilitate the investigation of the properties of these macromolecular aggregates, a detailed estimate of their interaction potential is inevitable. In general, the form of effective pair potential between these complex entities is determined by coarse-graining the intermolecular degrees of freedom. This allows one to represent each macromolecule as a single point section interacting via "ultra soft" potentials, where the overlap of the centers of mass of the macromolecules is feasible at a modest energy cost (~ kBT) without violating excluded volume interactions between monomers.

Recently, systems composed of ultrasoft colloidal sections have got much attention due to the richness of physics they offer as a consequence of the presence of at least one additional dimension (in the form of softness parameter) in the phase diagram . Among all the soft colloids, star polymers, dendrites and micro gels are the most studied soft colloidal systems. Various model potentials, such as Gaussian core , Yoshida Kamakura, Hertzian and harmonic spherical models have been used to describe the inter-psection interaction. Microgels are a class of soft colloids having usefull applications in several technological advancements such as nanotechnologies photonic crystals drug delivery systems food industry, water purification or chemical sensing , etc. They are hybrid units with a dual property, both of hard and soft psection , consisting of a mesoscopic cross-linked polymer network, which can deform, shrink or inter-penetrate with another microgel. Due to high responsiveness to external conditions (such as temperature or pH changes via adjusting their internal structure, microgels are considered smart materials. Apart from having industrial importance, the softness of these materials plays a fundamental role in determining overall physical properties and relative stability of various phases formed by them Early studies on the systems of microgels have attempted to derive the form of effective inter-psection interactions by resorting to an extreme coarse-graining approach by completely ignoring the internal structures by modeling the psections as hard spheres This approach is considered to be valid in the low temperature regime. However, it has been shown in recent studies that the interactions between microgels can be more accurately reproduced by a classic Hertzian repul sion , derived by computing the forces acting between two elastic spheres in the framework of classical elasticity theory . This approach leads to a monotonically decreasing purely repulsive power law potential with exponent equal to 5/2, describing the change in elastic energy of two deformable objects when subjected to an axial compression The potential has the following form

$$u(r) = \epsilon(1 - r/\sigma)^{\eta} \quad \text{for} \quad r < \sigma$$
$$= 0 \quad \text{for} \quad r \geq \sigma \qquad \text{.....1}$$

Berthier et al used liquid integral equation theory and molecular dynamics simulations to investigate the existence of amorphous glassy states in Hertzian colloids. Mohanty et alused experiment, theory, and simulation to study of the structural correlations between microgel

dispersions (both 2D and 3D) in the fluid phase in order to obtain the effective pair interaction potential between the microgels.

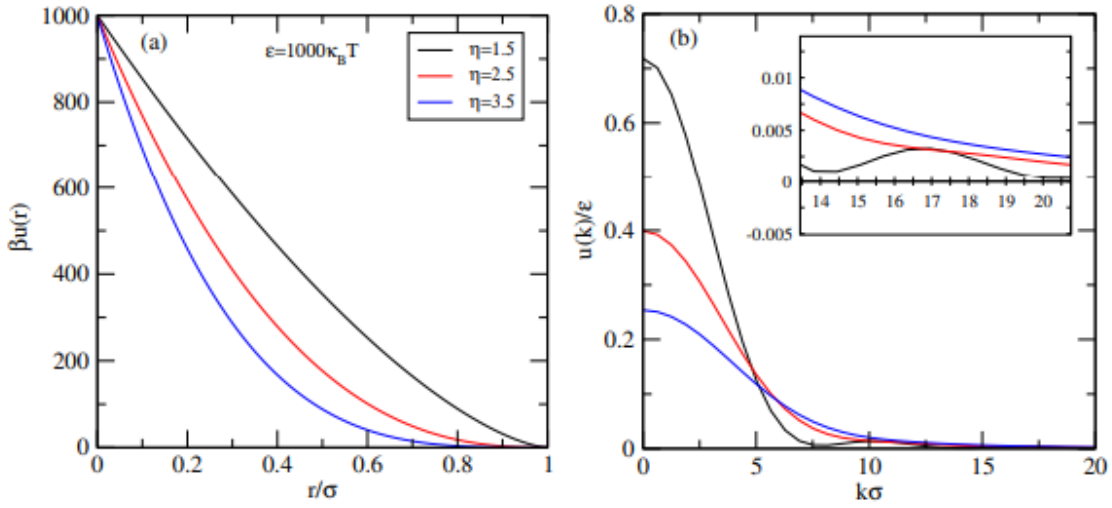

Figure 1: (a) Plot of potential at =1000kBT for the parameter η=3/2, 5/2 and 7/2. (b) 2D Fourier transform of the potential for the same set of parameters.

OBJECTIVE OF THE STUDY

1. To study on solid state band theory allows for the description of the behaviour of electrons in periodic lattices.

2. To study on Chern-Simons (CS) theories have the potential to reflect the universal low-energy picture of FQH physics

Pair Correlation Functions: Integral Equation Theory

The structure of an isotropic fluid is described by two psection density distribution function ρ (2)(r1, r2) because the single psection density distribution function, in this case, is a constant, independent of position and orientation. The two psection density distribution measures the probability of finding two psections simultaneously in an area element dA1 = dr1 (in 2D) around r1 and in the area element dA2 = dr2 around r2. The pair correlation function (PCF) g (2)(r1, r2), which is a central quantity in the theory of liquids, is related to two psection density distribution ρ (2)(r1, r2) as

$$g^{(2)}(\mathbf{r}_1, \mathbf{r}_2) = \frac{\rho^{(2)}(\mathbf{r}_1, \mathbf{r}_2)}{\rho^{(1)}(\mathbf{r}_1)\rho^{(1)}(\mathbf{r}_2)}. \quad \text{……..2}$$

In the case of a homogeneous isotropic fluid, the pair functions depends only on inter-psection distance |r1 −r2| = r12 Therefore, for isotropic fluid Eq. (3.2) becomes

$$\rho_f^2 g^{(2)}(r_{12}) = \rho^{(2)}(|\mathbf{r}_1 - \mathbf{r}_2|).$$ ……..3

The PCF g (2)(r12) ≡ g(r) are the lowest-order microscopic quantities which contain complete information about equilibrium structure of fluid along with having direct contact with the underlying interpsection interactions. It describes how psection density varies with distance and orientation with reference to a certain psection. Integral equation theory (IET) provide us a tool to evaluate the PCF as a function of position and thermodynamic parameters. IET involves, the solution of OrnsteinZernike equation(OZ) which connects total PCF h(r)[= g(r)−1] to another quantity c(r), called the two psection direct pair correlation function. In general OZ equation is written as

$$h(r) = c(r) - \rho \int h(r')c(r - r')d\mathbf{r},$$ …….4

which OZ involves two unknowns, namely h(r) and c(r), and therefore we need another equation to close the solution. The second equation, known as a closure relation, in general provides an approximate relation between PCFs and intermolecular interaction. It is the closure through which, interaction potential enters into the theory. Two extensively used closure equations in IET are, hypernetted chain (HNC) and Percus-Yevick (PY) closure, defined as

$$h(r) = \exp[-\beta u(r) + \gamma(r)] - 1$$ ……...5

$$h(r) = [\exp(-\beta u(r)) - 1](\gamma(r) + 1) + \gamma(r)$$ ……..6

where γ(r) = h(r) − c(r). OZ equation takes a particularly simple form in Fourier space, which is obtained by substituting the Fourier–Bessel transform of h and c functions, defined for any function f(r) in 2D as

$$f(k) = 2\pi \int_0^\infty dr r f(r) J_0(kr)$$ …….7

$$f(r) = \frac{2\pi}{(2\pi)^2} \int_0^\infty dk k f(k) J_0(kr),$$ …….8

where Jn(kr) are nth order Bessel function of first kind. Substituting Fourier transform of c(r) and h(r), gives rise to a simple algebraic equation

$$H(k) = C(k) + \rho C(k)H(k), \qquad \text{.....9}$$

RESEARCH METHODOLOGY

We consider a two-component system of total N spherical colloidal psections confined to a 2D plane of area A. Each component of the mixture is characterised by their diameters σa (large species, "a") and σb (small species, "b") and their partial number densities ρi = Ni/A. Psections interact via Hertzian model potential written as

$$u_{ij}(r_{ij}) = \epsilon_{ij}(1 - r_{ij}/\sigma_{ij})^{\eta} \quad \text{for} \quad r_{ij} < \sigma_{ij}$$
$$= 0 \quad \text{for} \quad r_{ij} \geq \sigma_{ij} \qquad \text{.....10}$$

where the indexes i, j = a, b refers to the psection species (a and b), rij is the centre to centre distance between the psections and σij = (σi + σj)/2. ij is the interaction strength parameter, which in this work has been taken to be identical for all the component pairs i.e. we choose a = ab = b = and define the scaled temperature as T ∗ = kBT/. η in the above expression is the tunable exponent which controls the shape of interaction. In the elastic case of small deformation its value is 5/2. In the present work, we have considered in addition to η = 5/2 and a slightly weaker case of η = 7/2. The psection of both the components are considered to differ in

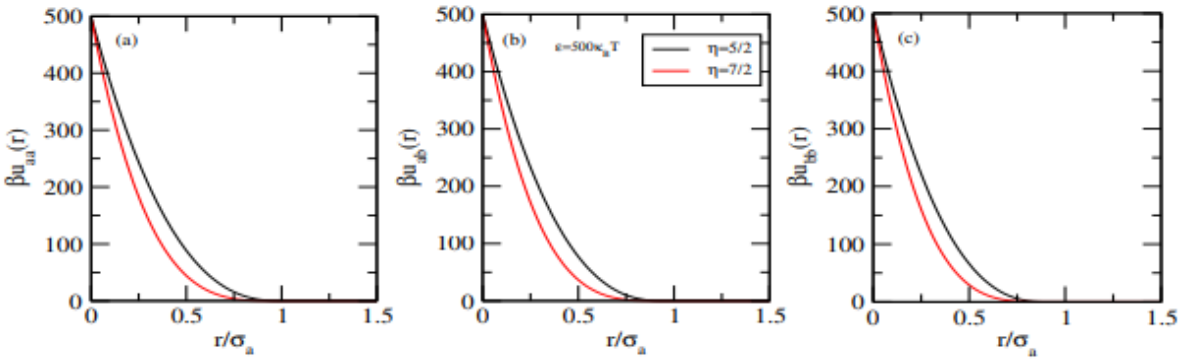

Figure 2: At 500 kBT, the interaction potential charts for the parameters η = 5/2 and 7/2 are as follows: (a) βuaa(r), (b) βuab(r), and (c) βubb(r).

their size slightly with the ratio σb/σa = 0.9. The diameter of the larger species σa has been taken as the characteristic length scale of the system and is used to scale all distances. In σa as the scaling parameter of the distance, we define reduced density as ρ ∗ = ρσ2 a . In, we have plotted the potential as a function of scaled inter psection separation r ∗ = r/σa at = 500kBT. We see here that for a given r/σa, the value of potential corresponding to higher exponent η is more steeper than that for the lower exponent. Potential remains finite even at r ∗ = 0 and become zero when the interpsection separation is larger than the corresponding effective diameter. It can be sheen that the interaction uaa survive a little longer than ubb. For simulation, we considered 500 number of psections, confined to a square box under periodic

boundary condition. Standard Metropolis Monte Carlo simulation has been carried out at a constant number of psections, volume and temperature. We have scaled the length of the simulation box by σa. The number of the psections of species a and b are determined by using the relation χa = Na/N and χb = Nb/N. Here Na and Nb are number of psections of species a and b respectively. N = Na + Nb, is the total number of psections.

RESULT

The results that we obtained from our density functional theory (DFT) calculation of the isotropic fluid-triangular solid freezing transition are presented in this part. Additionally, the phase diagram that corresponds to this transition is also shown in the T ∗ − ρ ∗ plane. In order for us to do this, we need the IET solution to be operating at much greater densities, close to the freezing transitions. In spite of this, it is well-known that HNC has a tendency to quantitatively underestimate the PCF at the high densities that were investigated in this study, as was discussed in section II. An elementary molecular dynamics (MD) simulation is carried out by us using 625 psections on a two-dimensional square lattice. The purpose of this simulation is to investigate the stability of HNC closure in the present system at higher densities. The box length and time were scaled in unit of σ and $\sqrt{m\sigma^2/k_BT}$ respectively. The total momentum was conserved by shifting the velocities of the psection. Velocity Verlet integration scheme was used to integrate Newton's equation of motion. The periodic boundary conditions were imposed in the usual fashion. The equilibrium condition was achieved by 106 time steps in NVE ensemble followed by another 106 runs to calculate the radial distribution function by , g(r) = $V/N^2\langle\sum_i\sum_{i\neq j}\delta(\mathbf{r}-\mathbf{r}_{ij})\rangle$. Here $\langle\cdots\rangle$ represents ensemble average over different configurations.

In we have compared g(r) curves obtained by HNC IET and MD simulation for the set of parameters $(\mathrm{a})\ \eta = 3/2,\ \epsilon = 100k_BT$ and $\rho^* = 1.30$; $(\mathrm{b})\ \eta = 5/2,\ \epsilon = 496k_BT$ and $\rho^* = 1.40$ and $(\mathrm{c})\eta = 7/2,\ \epsilon = 833k_BT$ and $\rho^* = 1.80$. As can be seen in this instance, HNC is capable of producing a first peak that is quantitatively accurate. Despite the fact that the subsequent peaks are less visible and underappreciated, it has been shown that they are qualitatively consistent with MD. Since the principal contributions to the DFT free energy come from the first few peaks of PCF, we believe that DFT will properly represent, at least qualitatively, the anticipated freezing transition parameters and the structure of the T − ρ ∗ phase diagram. This is because the DFT free energy is derived from the first few peaks of PCF.

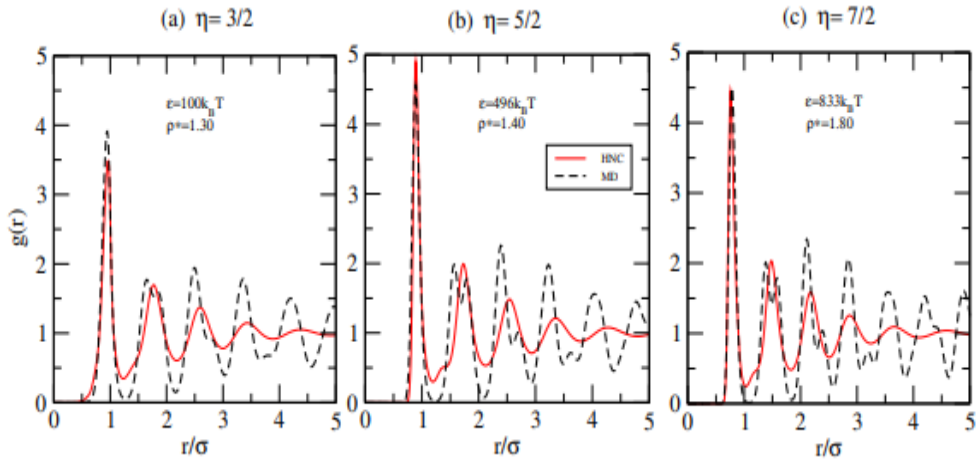

Figure 3 : Comparison of radial distribution functions g(r) obtained from HNC theory and MD simulation corresponding to exponent values

(a) $\eta = 3/2$ **for** $\epsilon = 100 k_B T$ **at** $\rho^* = 1.30$, **(b)** $\eta = 5/2$ **for** $\epsilon = 496 k_B T$ **at** $\rho^* = 1.40$ **(a)** $\eta = 7/2$ **for** $\epsilon = 833 k_B T$ **at** $\rho^* = 1.80$.

Table 1: Table for freezing transition parameters calculated for three different values of η. Here ϵ **represents the energy strength** T^* **represents the reduced temperature,** ρ_s^* **and** ρ_f^* **are the coexistence density of solid and fluid** α^* **is the localisation parameter and Lm is the relative displacement parameter.**

η	ϵ	T^*	ρ_l^*	ρ_s^*	α^*	$L_m = 2/\alpha^*$
3/2	89 *kBT* 100 *kBT* 125 *kBT*	0.0112 0.0100 0.0080	1.236 1.134 1.110	1.251 1.219 1.216	62.51 58.23 53.84	0.032 0.034 0.037
	333 k_BT	0.0030	1.53	1.54	35.22	0.056
5/2	496 *kBT*	0.00201	1.31	1.40	39.09	0.051
	1000 *kBT*	0.0010	1.18	1.33	43.07	0.046
	714 k_BT	0.0014	1.868	1.877	31.51	0.063
7/2	830 k_BT	0.0012	1.726	1.746	32.74	0.061
	1000 k_BT	0.0010	1.630	1.659	33.72	0.059

In we have presented the $T^* - \rho^*$ phase diagram for all the three systems under consideration. In the case of η = 3/2, the system is always fluid for $T^* > 0.0115(\epsilon < 87).$ At a smaller T^* (larger ϵ) value, system transform from fluid to solid as we increase the density. The solid is found to be stable in the range $T^* = 0.007; \rho^* = 1.213$ to $T^* = 0.0115; \rho^* = 1.283,$ in our calculation. When the temperature increases, the gap that separates the solidus and liquidus lines becomes shorter. The coexistence zone is traversed by a tie line that is parallel to the axis. As the value of T grows, the tie line becomes narrower, indicating a change from fluid behaviour to solid behaviour. At a temperature of ρ ∗ less than 1.213, we made the discovery that a fluid cannot be transformed into a solid by lowering its temperature. illustrates the phase diagram with the value of η equal to 5/2, which shows a nature that is comparable. However, in this particular case, the range of stable solid is from T ∗ = 0.001; ρ ∗ = 1.33 to T ∗ = 0.003; ρ ∗ = 1.60. By lowering the temperature below ρ ∗ = 1.33, we were unable to achieve the desired result of the fluid becoming solid. Additionally, in contrast to the previous case, the region that is between the liquidus and solidus lines comprises a smaller territory. On the other hand, when the value of η is set to 7/2, the phase diagram becomes even more constrained, resulting in the identification of a stable solid within the range of T ∗ = 0.001; ρ ∗ = 1.67 to T ∗ = 00148; ρ ∗ = 1.98. When the exponent η is raised in each of the three instances, the topology of the phase diagram takes on the distinctive shape of the temperature-density phase diagram of a simple liquid. This phase diagram often contains a fluid-solid coexistence region that decreases as the potential gets more soft.

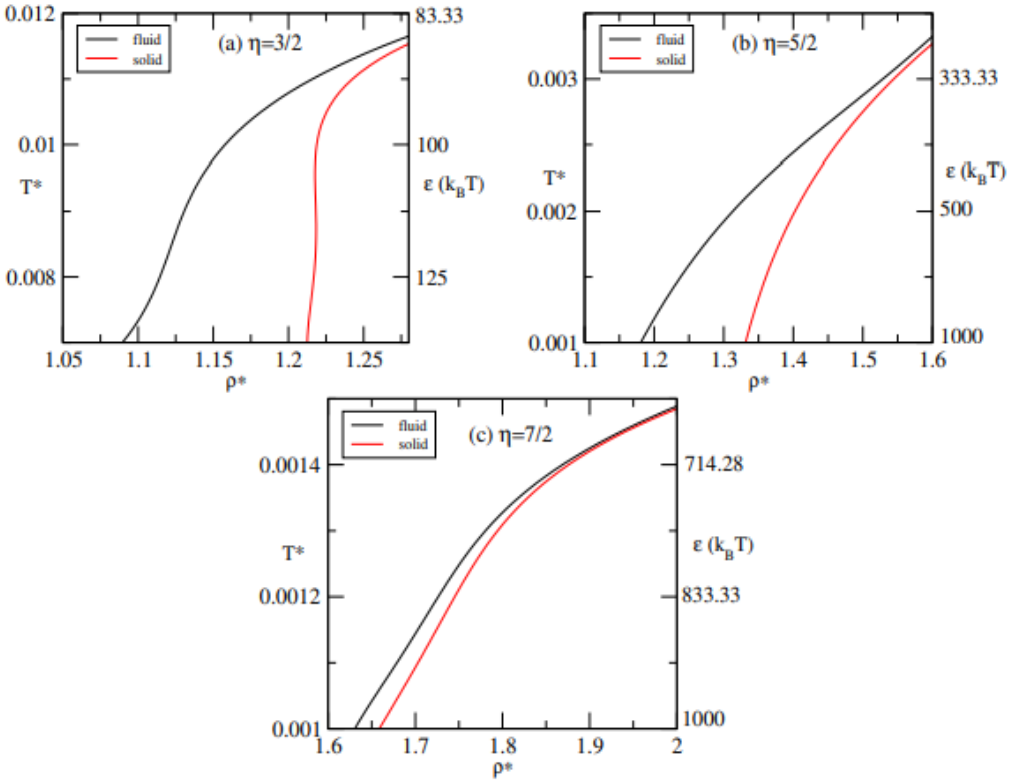

Figure 4: The phase diagram in temperature-density plane for the Hertzian type interaction potential corresponding to the exponent (a) η = 3/2, (b) η = 5/2 and (c) η = 7/2.

Table 2 : Table for freezing parameters

Methods	**Tilt angle** ϕ	Γ_f	Γ_s	α^*
Experiment	90°	10.0	9.3	
Simulation	90°	10.75	9.49	
MWDA with RY closure	90°	41.07	41.13	
	90°	42.3458	42.3557	279.10
RY DFT with HNC				
	85°	43.5493	43.5512	290.10
	80°	47.7552	47.7670	339.05
	75°	66.8076	66.8198	625.10

In order to evaluate the fluid-triangular solid freezing transition parameters, we will now use the RY DFT technique. This will be done in the subsequent sections, specifically for systems with tilt angles of φ = 850, 800, and 750. HNC integral equation theory provides the structural inputs for this assessment in the form of c(k). These inputs are used to evaluate the structure. Calculating the transition parameters at the coexistence is accomplished by the use of the same tangent construction technique that was discussed. The first stage in our one-component system scenario is determining the total free energy of the fluid phase (Ff) and the solid phase (Fs) as a function of Λ. This may also be referred to as the global minimum of the ΔF-α ∗ curve. The total free energy of the fluid phase, denoted by Ff, is obtained by first integrating the compressibility pressure which is measured at a grid of. After that, it is replaced in order to acquire the excess free energy contribution of the fluid, and the ideal gas contribution that corresponds to it is then taken into account. After that, the total free energy of the solid Fs is obtained by adding Ff to the ΔF that corresponds to the global minimum. Next, a figure is generated by plotting these free energy densities, which are denoted as Ff /A and Fs /A, against the average density, which is denoted as ρ(∝ Γ 2/3). Using a tangent that is shared by both curves, the values of Γ2/3 s and Γ 2/3 f, as well as the freezing and melting

densities that are associated with them, ρs and ρf, may be derived.

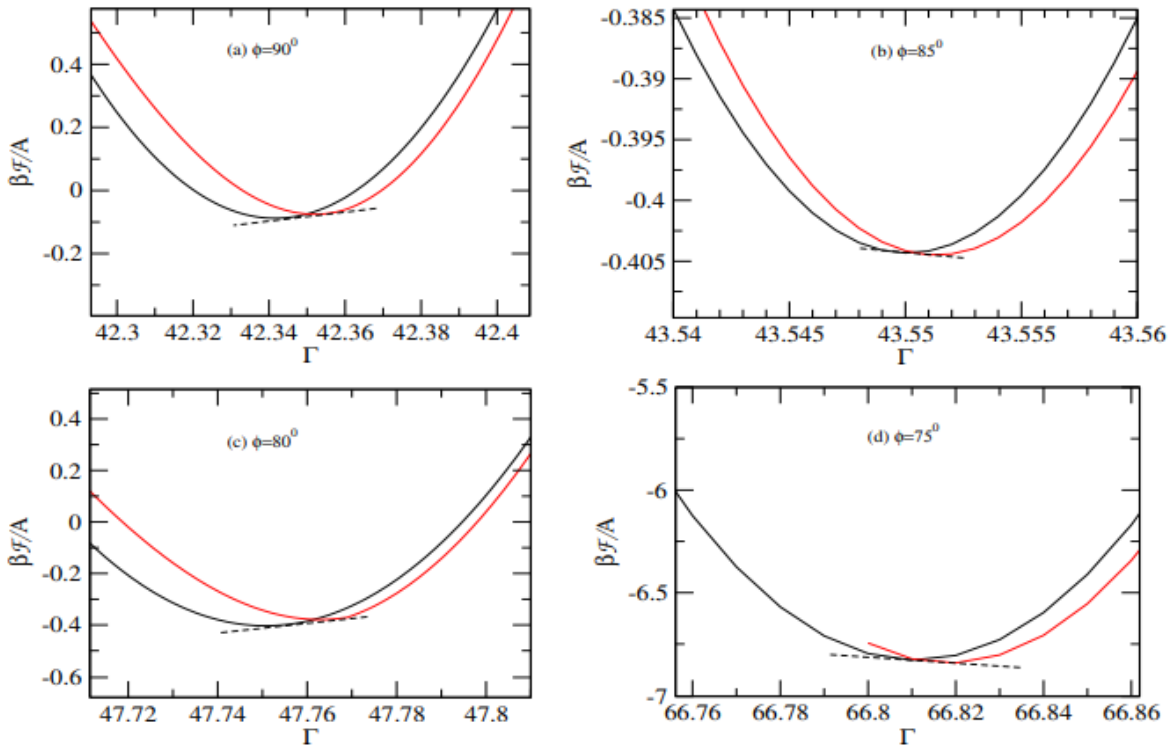

Figure 5: Plot of the free energy density of fluid Ff /A(black curve) and solid Fs/A (red curve) as a function of Γ. The common tangent to the curves has also been shown in the figure.

Table 4.3 : Table for freezing parameters

ϕ	Γ_f	Γ_s	α^*	L_m
90°	14.6297	14.6303	160.00	0.0125
85°	15.6892	15.6908	168.08	0.0118
80°	22.6130	22.6236	330.00	0.0060

In we have plotted the free energy densities βFf /A and βFs/A as a function of Γ. The tangent to the curves are also shown in the figure. In we have enlisted the transition parameters Γs and Γf for φ = 900 , 850 and 800 . Here we have also listed the modified Lindeman parameter defined as Lm = $\sqrt{\langle(\Delta\mathbf{r}_i - \Delta\mathbf{r}_{i+1})^2\rangle}/a$ where i and i + 1 are the nearest neighbor in the 2D lattice. Since the nearest-neighbor correlations $\langle\mathbf{r}_i \cdot \mathbf{r}_{i+1}\rangle$ are expected to be positive:

$$L_m \lesssim 2\langle \mathbf{r}_i^2 \rangle / a \approx 2/(\alpha_{\min} a^2) = 2/\alpha^*$$

With regard to the relative displacement parameter L c m, it has been said that the critical value at which a two-dimensional solid begins to melt is 0.033. The table makes it abundantly evident that the values of matching Γ at the coexistence increase as the tilt angle of the axially symmetric quadruples lowers. Given the way that the tilt angle influences PCFs, this makes perfect logic. In addition, a low value for the relative displacement parameter $\alpha*$ is indicative of the fact that the RY DFT overestimates the localization.

CONCLUSION

In the course of our investigation into this topic, we are embarking on a journey of discovery, and if everything goes according to plan, we will find new vistas and get a whole different point of view on the universe. Two-dimensionally limited spherical ultra-soft colloids were the subject of this investigation, and the purpose of the research was to investigate the pair structures and freezing transitions that occur inside the system. The hyper netted chain integral equation theory and the density functional theory of freezing were both used in our approach, which enabled us to accomplish this. There are three different interaction potentials that are investigated within the framework of the Hertzian type model here. These include an elastic Hertzian potential with an exponent of η = 5/2, an interaction potential that is considerably more difficult to deal with with η = 3/2, and an interaction that is notably simpler to deal with with η = 7/2. Based on the findings, it can be shown that the pair correlation functions of the system, which correspond to the three different interaction situations, are significantly different from one another. In order to calculate these functions, a grid of system parameters, which includes measurements of temperature and density, is used.

REFERENCE

[1] Levin, Michael; Wen, Xiao-Gang (2005). "Colloquium: Photons and electrons as emergent phenomena". Reviews of Modern Physics. 77 (3): 871–879.

[2] Jump up to:a b Neil W. Ashcroft; N. David Mermin (1976). Solid state physics. Saunders College.

[3] Eckert, Michael (2011). "Disputed discovery: the beginnings of X-ray diffraction in crystals in 1912 and its repercussions". Acta Crystallographica A.

[4] Han, Jung Hoon (2010). Solid State Physics (PDF). Sung Kyun Kwan University. Archived from the original (PDF) on 2013-05-20.

[5] Jump up to:a b Perdew, John P.; Ruzsinszky, Adrienn (2010). "Fourteen Easy Lessons in Density Functional Theory" (PDF). International Journal of Quantum Chemistry. 110 (15): 2801–280. Archived (PDF) from the original on 2022-10-09. Retrieved 13 May 2012.

[6] Nambu, Yoichiro (8 December 2008). "Spontaneous Symmetry Breaking in Psection Physics: a Case of Cross Fertilization".

[7] Greiter, Martin (16 March 2005). "Is electromagnetic gauge invariance spontaneously violated in superconductors?.

[8] Jump up to:a b Vojta, Matthias (2003). "Quantum phase transitions". Reports on Progress in Physics.

[9] Malcolm F. Collins Professor of Physics McMaster University (1989-03-02). Magnetic Critical Scattering.

[10] Richardson, Robert C. (1988). Experimental methods in Condensed Matter Physics at Low Temperatures. Addison-Wesley.

[11] Jump up to:a b Chaikin, P. M.; Lubensky, T. C. (1995). Principles of condensed matter physics. Cambridge University Press. ISBN 978-0-521-43224-5.

[12] Wentao Zhang (22 August 2012). Photoemission Spectroscopy on High Temperature Superconductor: A Study of Bi2Sr2CaCu2O8 by Laser-Based Angle-Resolved Photoemission. Springer Science & Business Media. .

[13] Siegel, R. W. (1980). "Positron Annihilation Spectroscopy". Annual Review of Materials Science. 10: 393–425.

[14] Committee on Facilities for Condensed Matter Physics. The magnetic field is not simply a spectroscopic tool but a thermodynamic variable which, along with temperature and pressure, controls the state, the phase transitions and the properties of materials.

[15] Jump up to:a b Committee to Assess the Current Status and Future Direction of High Magnetic Field Science in the United States; Board on Physics and Astronomy; Division on Engineering and Physical Sciences; National Research Council (25 November 2013). High Magnetic Field Science and Its Application in the United States: Current Status and Future Directions.

[16] Moulton, W. G.; Reyes, A. P. (2006). "Nuclear Magnetic Resonance in Solids at very high magnetic fields". In Herlach, Fritz (ed.). High Magnetic Fields. Science and Technology.

[17] Doiron-Leyraud, Nicolas; et al. (2007). "Quantum oscillations and the Fermi surface in an underdoped high-Tc superconductor".

[18] Greiner, Markus; Fölling, Simon (2008). "Condensed-matter physics: Optical lattices".

[19] Jaksch, D.; Zoller, P. (2005). "The cold atom Hubbard toolbox". Annals of Physics.

[20] Glanz, James (October 10, 2001). "3 Researchers Based in U.S. Win Nobel Prize in Physics". The New York Times. Retrieved 23 May 2012.

[21] Committee on CMMP 2010; Solid State Sciences Committee; Board on Physics and Astronomy; Division on Engineering and Physical Sciences, National Research Council.

[22] Jump up to:a b c Yeh, Nai-Chang (2008). "A Perspective of Frontiers in Modern Condensed Matter Physics" (PDF). AAPPS Bulletin. 18 (2). Retrieved 19 June 2018.

[23] Kudernac, Tibor; Ruangsupapichat, Nopporn; Parschau, Manfred; Maciá, Beatriz; Katsonis, Nathalie; Harutyunyan, Syuzanna R.; Ernst, Karl-Heinz; Feringa, Ben L.

[24] López, A., and Fradkin, E. 1999. Universal structure of the edge states of the fractional quantum Hall states. Phys. Rev. B, 59, 15323.

[25] López, A., and Fradkin, E. 2001. Effective field theory for the bulk and edge states of quantum Hall states in unpolarized single layer and bilayer systems. Phys. Rev. B, 63, 085306.